Radiation Physics and Chemistry 215 (2024) 111367

Contents lists available at ScienceDirect

Radiation Physics and Chemistry

journal homepage: www.elsevier.com/locate/radphyschem

Scintillation property of Tl-doped NaI transparent ceramics

Yuta Yoshikawa *, Takumi Kato, Daisuke Nakauchi, Noriaki Kawaguchi, Takayuki Yanagida

Nara Institute of Science and Technology (NAIST), 8916-5, Takayama-cho, Ikoma-shi, Nara, 630-0192, Japan

ARTICLE INFO

Handling Editor: Dr. Chris Chantler

ABSTRACT

In this study, Tl-doped NaI transparent ceramics with varying doping concentrations (0.05, 0.1, 0.3, and 0.5%) were synthesized using the spark plasma sintering (SPS) method, and We investigated the optical and scintillation properties. In terms of optical properties, the 0.1% Tl-doped NaI sample showed the diffuse transmittance of ~70% in the visible range. The photoluminescence peak was observed at around 420 nm with the decay time of approximately 150 ns. The scintillation peak was also observed at 420 nm due to $^3P_1 \rightarrow {}^1S_0$ transition of Tl^+. In addition, all the samples showed the scintillation peak at 330 nm due to self-trapped exciton. Among all the samples, the 0.1% Tl-doped NaI sample showed the highest light yield (36,000 ph/MeV) under ^{137}Cs γ-ray irradiation, and this value is almost equivalent to that of Tl-doped NaI single crystals (38,000 ph/MeV).

1. Introduction

Scintillators are the type of phosphors that immediately convert ionizing radiations such as X- and γ-rays into visible photons by interactions of ionizing radiation with materials. Therefore, scintillators have been applied in multiple fields, such as environmental monitoring (Watanabe et al., 2015), security (Paepen et al., 2013), medical (Van Eijk, 2003), biology (Matsubara et al., 2021), resource exploration (Yanagida et al., 2013a), and astrophysics (Bloser et al., 2014). In general, high scintillation light yield (*LY*), rapid decay of scintillation, low afterglow level (*AL*), and high effective atomic number were required for X- and γ-ray measurements. However, no scintillators can completely meet all the required specifications. Therefore, users are required to select an appropriate scintillator from the existing options, taking into consideration the specific application. As a result, numerous researchers have continued to look for new desirable materials (Yanagida, 2018).

Among them, single crystal scintillators have been used most widely because of their high transparency. However, single crystals generally have some disadvantages. For example, the fabrication of single crystals is quite time-consuming, and they are also difficult to produce in a large size, which leads to high costs. However, recent advancements in sintering technology have enabled the synthesis of ceramics with high transparency. As a result, transparent ceramics are anticipated to find practical applications in the field of scintillators (Greskovich and Duclos, 1997). Transparent ceramics not only overcome the mechanical strength and cost problems of single crystals but also has the potential to become high-performance scintillators over conventionally used single crystals.

In previous studies on transparent ceramics scintillators, garnet oxides and halides except iodide have been reported intensively (Yanagida et al., 2005, 2011; Seeley et al., 2013; Cherepy et al., 2010; Kato et al., 2017, 2018; Kimura et al., 2018, 2019). Especially, the transparent ceramics such as $Ce:Gd_3Al_2Ga_3O_{12}$ (Yanagida et al., 2013b), $Pr:Lu_3Al_5O_{12}$ (Yanagida et al., 2012), and $Ce:Lu_3Al_5O_{12}$ (Yanagida et al., 2011) showed higher scintillation *LY* than that of the single crystal with the same chemical composition.

In this study, we focused on NaI transparent ceramics as a new material form. Tl-doped NaI single crystal scintillator was found by Hofstadter in 1948 (Hofstadter, 1948) (Hofstadter and McIntyre, 1950), and it has been the most common scintillator for a long time (Phenomena et al., 1953; Sibczyński et al., 2012; Sailer et al., 2012; Robertson and Lynch, 1961; Alexandrov et al., 2008; Ishikane, 1974). Tl-doped NaI single crystal scintillator is characterized by relatively high *LY* (~38,000 photon/MeV) (Lecoq, 2016), low cost of raw powder, and high γ-ray sensitivity because blue emission peak (415 nm) of Tl^+ is suitable for the common photomultiplier response. Thus, they are still widely applied to experiments in nuclear physics, environmental radiation measurements, and medical fields. However, no research regarding the scintillation properties of Tl-doped NaI transparent ceramics has been reported. Thus, Tl-doped NaI transparent ceramics were fabricated by the spark plasma sintering (SPS) method, and optical and scintillation properties were evaluated to investigate the potential of transparent ceramics as an alternative material to single crystals.

* Corresponding author.
E-mail address: yoshikawa.yuta.yv5@ms.naist.jp (Y. Yoshikawa).

https://doi.org/10.1016/j.radphyschem.2023.111367
Received 21 August 2023; Received in revised form 27 September 2023; Accepted 24 October 2023
Available online 28 October 2023

2. Experimental procedure

2.1. Sample preparation

Tl-doped NaI transparent ceramics with various concentrations of Tl^+ (0.05, 0.1, 0.3, and 0.5%) were synthesized by the SPS method (LABOX-110, Sinterland) using NaI (99.999%, Sigma-Aldrich) and TlI (99.999%, Sigma-Aldrich) raw powders. The raw powders were mixed inside a glove box with less than 20% humidity under a nitrogen atmosphere, and the mixed powder was subsequently dried at 400 °C for 4 h under vacuum conditions.

A sintering was performed under vacuum by the following condition. The sintering temperature was increased from 20 °C to the target temperature of 450 °C at a rate of 10 °C/min and then held for 15 min while applying a pressure of 45 MPa. After synthesis, the surfaces of all the samples were polished by 300–3000 grid sandpapers.

2.2. Optical properties

Regarding the optical properties, we used the following equipment to measure the diffuse transmittance spectra, photoluminescence (PL) spectra, PL quantum yields (*QY*), and PL decay curves: a spectrophotometer (SolidSpec-3700, Shimadzu) for the diffuse transmittance spectra, spectrofluorometer (FP-8600, JASCO) for the PL spectra, Quantaurus-QY (C11347, Hamamatsu) for the *QY*, and Quantaurus-τ (C11367, Hamamatsu) for the PL decay curves.

2.3. Evaluation of scintillation properties

In order to investigate the scintillation properties, we conducted measurements of X-ray-induced scintillation spectra, scintillation decay curves, afterglow profiles, and pulse height spectra using our original setup (Yanagida et al., 2013b) (Yanagida et al., 2014a). In the pulse height spectra, ^{137}Cs was used as the γ-ray source, and the relative *LY*s of the samples were determined by comparing them with the calibrated scintillator Gd_2SiO_5:Ce (GSO:Ce), which has an absolute *LY* of 8,000 photons/MeV. These scintillation properties were measured in the same way as in our previous study (Yoshikawa et al., 2022).

3. Results and discussion

3.1. Samples

Fig. 1 shows the photographs of the Tl-doped NaI transparent ceramics under room light (lower part) and UV light (upper part). All the samples were polished to adjust their thickness to 1 mm. In comparison with the undoped NaI transparent ceramic (Yoshikawa et al., 2022), no coloring by Tl-doping was seen. Moreover, all the samples were transparent in the visible range, and letters on the reverse side were clearly visible. Under UV light, blue luminescence from Tl-doped NaI transparent ceramics was observed.

3.2. Optical properties

Fig. 2 illustrates the spectra of diffuse transmittance of the Tl-doped NaI samples. All the samples had an absorption band at around 260 nm. Although experimental data regarding the bandgap of NaI was not found, a simulation estimated the bandgap to be approximately 5 eV (Messaoudi et al., 2015).

Our result that the absorption band was observed at 260 nm (~4.7 eV) roughly agreed with the simulation. In addition, our previous study about undoped NaI transparent ceramics reported the same absorption (Yoshikawa et al., 2022). Thus, a strong absorption bands below 260 nm did not depend on Tl^+ ions but on NaI host. Apart from this absorption, the Tl-doped NaI samples showed an absorption band at around 300 nm, of which the origin would be $^1S_0 \rightarrow {}^3P_1$ transition of Tl^+ (Van Sciver, 1956). The transmittance in the range of 320–450 nm decreased with increasing Tl concentration, which is attributed to Tl_2^* (Ershov et al., 1994). The significant decrease in the transmittance of the 0.5% Tl-doped NaI sample would be due to an increase in scattering centers.

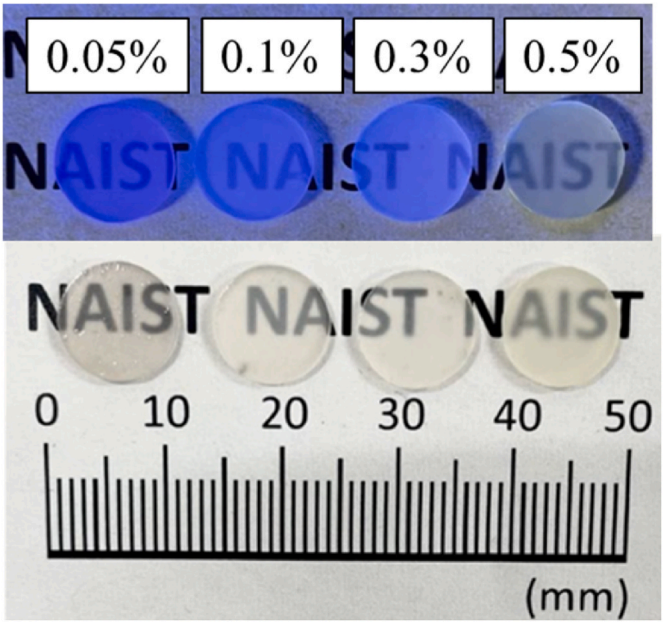

Fig. 1. Photographs of the Tl-doped NaI transparent ceramics under room light (lower part) and UV light (upper part).

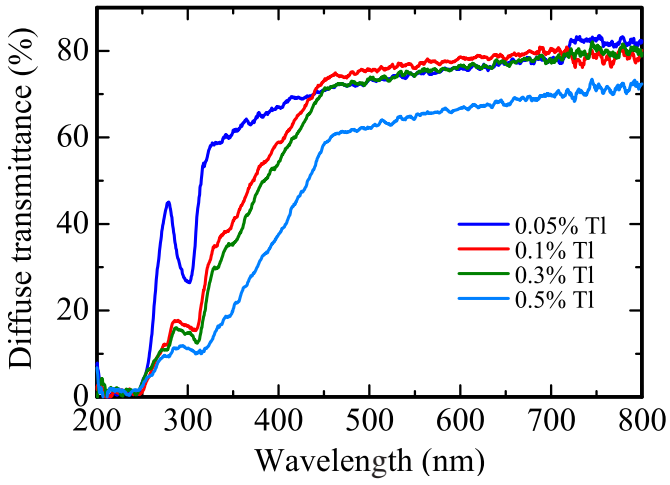

Fig. 2. Diffuse transmittance spectra of the Tl-doped NaI samples.

PL excitation/emission spectra of the Tl-doped NaI samples are shown in Fig. 3. By excitation at 285 nm, an emission peak was observed at around 420 nm for the 0.05, 0.1, and 0.3% Tl-doped NaI samples, while the 0.5% Tl-doped sample showed an emission peak at ~450 nm. The shift of the emission peak in the 0.5% Tl-doped sample would be due to decreased transparency and increased self-absorption at the emission wavelength, which could be confirmed by Fig. 2. The emission peaks at 420–450 nm are caused by $^3P_1 \rightarrow {}^1S_0$ transition of Tl^+ because a similar emission peak has been reported for Tl-doped NaI single crystal (Van Sciver, 1956). The PL *QY*s of 0.05, 0.1, 0.3, and 0.5% Tl-doped NaI samples were 44, 48, 42, and 21%, respectively. The PL *QY* became maximum at Tl concentration of 0.1% and decreased above 0.3% because of concentration quenching.

The PL decay curves of the Tl-doped NaI samples monitored at 415 nm under 280 nm excitation are shown in Fig. 4. The decay curves were

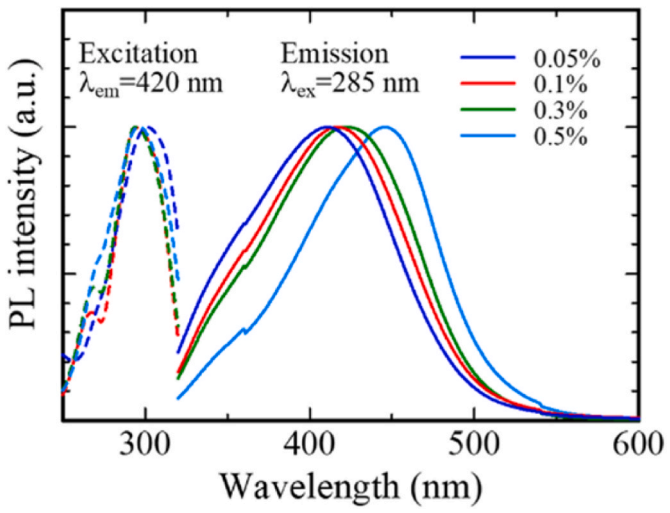

Fig. 3. PL excitation/emission spectra of the Tl-doped NaI samples. The PL intensities were normalized to maximum values. The intensity was normalized at emission peak wavelength.

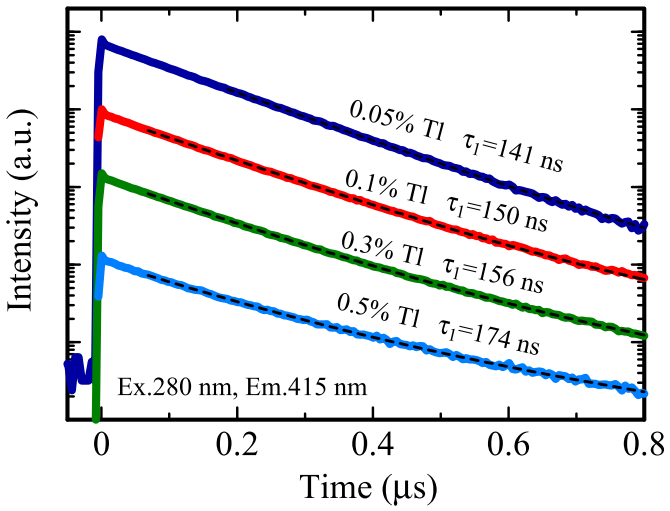

Fig. 4. PL decay curves of the Tl-doped NaI samples. The dashed lines indicate fitting profiles. The monitoring emission wavelength was 415 nm and the excitation wavelength was 280 nm.

approximated by a single exponential function, resulting in PL decay time constants. The decay time constant of the 0.05, 0.1, 0.3, and 0.5% Tl-doped NaI samples were 141, 150, 156, and 174 ns, respectively. These values are general as $^3P_1 \rightarrow {}^1S_0$ transition in Tl-doped alkali halide and roughly similar to those of Tl-doped NaI single crystals (Ishikane and Kawanishi, 1975).

3.3. Scintillation properties

Fig. 5 exhibits X-ray-induced scintillation spectra of the Tl-doped NaI samples. We observed scintillation peaks at 330 and 420 nm in the 0.05% Tl-doped sample, whereas scintillation peaks of the other samples were observed at 330 and 450 nm. The redshift from 420 to 450 nm was observed as with the PL spectra. This would be due to decreased transparency and increased self-absorption at the emission wavelength. Since the geometry of scintillation spectra was transmission-type while that of PL was reflection-type, scintillation spectra suffered more by the self-absorption. The scintillation peak at 330 nm was reported to be attributed to self-trapped exciton (STE) (Nagata et al., 1990). This peak was

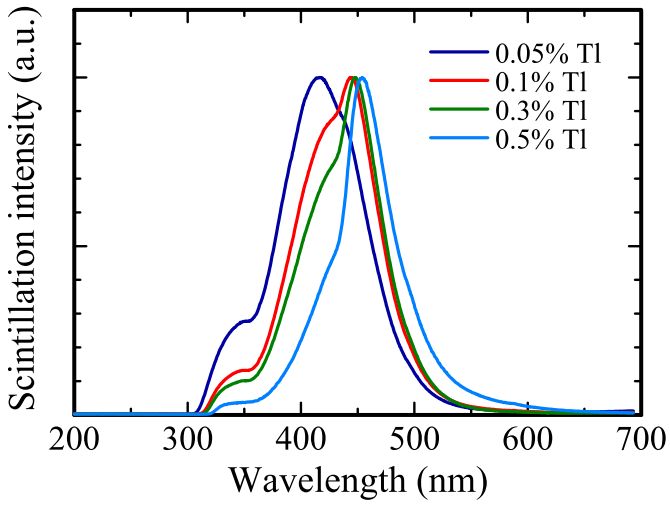

Fig. 5. Scintillation spectra of the Tl-doped NaI samples induced by X-rays. The scintillation intensities were normalized at their peak emission wavelength. The intensity was normalized at emission peak wavelength.

also observed in the undoped NaI transparent ceramics in the previous study (Yoshikawa et al., 2022). The scintillation peak at 420–450 nm was ascribed to $^3P_1 \rightarrow {}^1S_0$ transition of Tl^+ since the wavelength was almost the same as PL and the past report (Van Sciver, 1956).

Fig. 6 exhibits the scintillation decay curves of the Tl-doped NaI samples. The decay curves were approximated by a single exponential function. The decay time constants of the 0.05, 0.1, 0.3, and 0.5% Tl-doped NaI samples were 176, 205, 220, and 259 ns, respectively. Considering the PL properties and scintillation spectra, these decay time constants are attributed to $^3P_1 \rightarrow {}^1S_0$ transition of Tl^+. However, scintillation decay times were longer than PL decay times. This difference may be due to the fact that scintillation has a complex mechanism involving a transfer process from the host to the luminescent center, whereas PL is observed as a consequence of excitation and subsequent radiative relaxation of the localized luminescent center. We think that the longer scintillation decay time constant compared to the PL decay time constant is primarily due to the involvement of energy transfer processes. Further, the observed scintillation decay times were close to that of common Tl-doped NaI single crystal scintillator (~230 ns) (Shiran et al., 2010).

In addition, we observed a significant difference in the rise part when

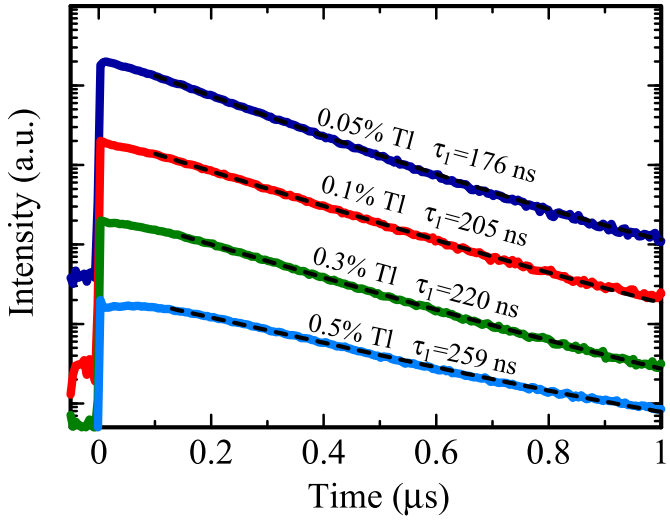

Fig. 6. Scintillation decay curves of the Tl-doped NaI samples induced by X-rays. The dashed lines indicate fitting profiles.

compared with PL decay curves. The rise was very fast in the PL decay curves, while that in scintillation was very slow, and flat shapes (in other words, slow rise) were observed in the scintillation decay curves, especially in Tl densely doped samples. Such a shape of the scintillation decay curves has also been reported in Tl-doped NaI single crystals (Kubota et al., 1998). The flat shapes of the decay curve are interpreted to be due to the sum of the scintillation photons from prompt processes which is the energy transfer from the host directly to Tl^{+} centers and diffusion process which is the energy transfer from Tl^{0} and V_k center pairs to the Tl^{+} center (Kubota et al., 1998).

Fig. 7 shows the afterglow (*AL*) curves of the Tl-doped NaI samples after X-ray irradiation for 2 ms. Here, the *AL* is defined by $AL\ [\%] = (I_2–I_0)/(I_1–I_0) \times 100$, where I_0 is the background signal intensity, I_1 is the averaged signal intensity under X-ray exposure, and I_2 is the signal intensity at 20 ms after X-ray irradiation. The *AL*s at 20 ms of the 0.05, 0.1, 0.3, and 0.5% Tl-doped NaI samples were 0.08, 0.17, 0.29, and 1.08%, respectively. The *AL*s were found to increase as the Tl concentration increased. According to the previous study in Tl-doped CsI (Bartram et al., 2006), it was concluded that the increase in the *AL*s was attributed to the radiative recombination of trapped holes and thermal ionized Tl^{0} at room temperature. Thus, analogically with Tl-doped CsI, *AL*s of the Tl-doped NaI samples would increase with increasing Tl concentration. The *AL*s obtained in this study were higher than that of Tl-doped CsI single crystal (0.04%) measured in the same setup (Takahashi et al., 2020). This result suggests that the Tl-doped NaI transparent ceramics include more defects corresponding to shallow trap levels that can be thermally stimulated at room temperature than Tl-doped CsI single crystal.

Fig. 8 shows the pulse height spectra of the Tl-doped NaI samples using the radioisotope of ^{137}Cs. In all the spectra, the photoabsorption peaks could be observed. The peaks of the Tl-doped NaI samples with Tl concentrations of 0.05, 0.1, 0.3, and 0.5% were observed at the MCA channels of 471, 577, 432, and 236, respectively. The photoabsorption peak of the GSO:Ce scintillator (8,000 photons/MeV) appeared at 118. Here, quantum efficiencies (*QE*) of the PMT were considered for the emissions at 420 nm ($QE_{420} = 36\%$ for the emission of Tl-doped NaI) and at 440 nm ($QE_{440} = 33\%$ for the emission of GSO:Ce). Based on the photoabsorption peaks and *QE*s, the *LY*s of the 0.05, 0.1, 0.3, and 0.5% Tl-doped NaI samples were calculated to be 29,000, 36,000, 27,000, and 15,000 photons/MeV with a typical error of ±10%, respectively. These values in addition to *QY*s and *AL*s were listed in Table 1. Among the samples, the 0.1% Tl-doped NaI sample showed the highest *LY* (~36,000 photons/MeV) which was almost equivalent to that of commercial Tl-doped NaI single crystal (38,000 photons/MeV) (Weber, 2002). It has also been reported that the optimum Tl concentration for Tl-doped NaI single crystal scintillator was determined to be approximately 0.1–0.2% (Murray and Meyer, 1961). The report is consistent with the optimum Tl concentration of NaI samples in this study.

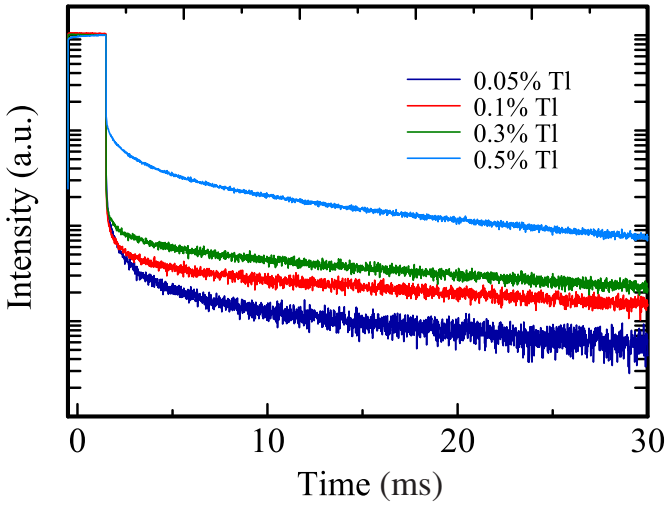

Fig. 7. Afterglow curves of the Tl-doped NaI samples induced by X-ray.

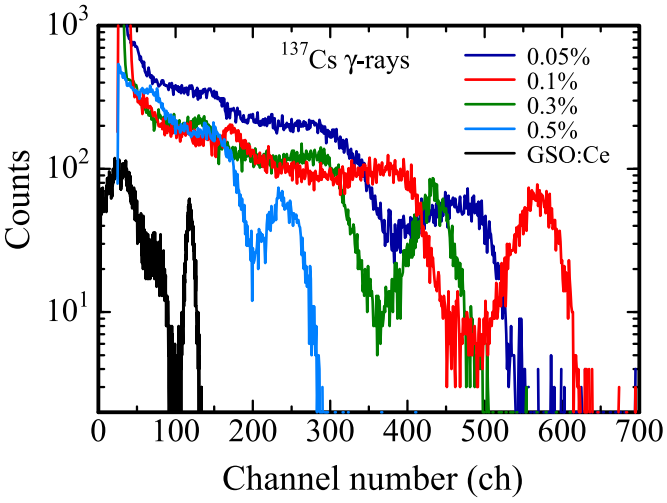

Fig. 8. Pulse height spectra of Tl-doped NaI samples under γ-ray irradiation from ^{137}Cs. The spectrum of GSO:Ce is also shown as a reference.

Table 1
*QY*s, *AL*s, and *LY*s of Tl-doped NaI samples.

Samples	*QY* (%)	*AL* (%)	*LY* (photons/MeV)
0.05% Tl	44	0.08	29,000
0.1% Tl	48	0.17	36,000
0.3% Tl	42	0.29	27,000
0.5% Tl	21	1.08	15,000

On the other hand, the *AL*s suggest that the Tl-doped NaI samples have some defects, which have the role of trapping centers. The main reason for this may be that the SPS method is generally a highly reductive fabrication technique, resulting in anions (I^{-}) and other defects in the samples fabricated by SPS. Recently, it has been revealed that the connection between scintillation and the number of trapping centers is inversely proportional (Yanagida, 2016) (Yanagida et al., 2014b). In future work, if the sintering condition in the SPS process and the dry process of raw powders are optimized, the transparent ceramics may show higher *LY* than the commercial Tl-doped NaI single crystal scintillator by decreasing trapping centers.

4. Conclusion

We have successfully synthesized 0.05, 0.1, 0.3, and 0.5% Tl-doped NaI transparent ceramics using the SPS method. Under X-ray irradiation, all the samples showed scintillation peaks at 330 and 420 nm. These peaks are due to STE and $^3P_1 \rightarrow {}^1S_0$ transition of Tl^{+} ions. When irradiated by ^{137}Cs γ-rays, the pulse height spectra showed that the 0.1% Tl-doped NaI sample had the highest *LY* among all the samples (36,000 ph/MeV). This value is almost equivalent to that of Tl-doped NaI single crystal (38,000 ph/MeV). Therefore, the Tl-doped NaI transparent ceramics scintillator can replace Tl-doped NaI single crystals scintillator which is currently used.

Credit author statement

All persons who meet authorship criteria are listed as authors, and all authors certify that they have participated sufficiently in the work to take public responsibility for the content.

1. Yuta Yoshikawa: Investigation, Writing-original draft preparation.
2. Takumi Kato: Conceptualization, Validation, Writing-Review, and

Editing.

3. Daisuke Nakauchi: Supervision.

4. Noriaki Kawaguchi: Funding acquisition, Supervision.

5. Takayuki Yanagida: Writing-Review and Editing, Funding acquisition, Project administration.

Declaration of competing interest

The authors declare that they have no known competing financial interests or personal relationships that could have appeared to influence the work reported in this paper.

Data availability

No data was used for the research described in the article.

Acknowledgments

This work was supported by Grants-in-Aid for Scientific A (22H00309), Grants-in-Aid for Scientific B (22H03872, 22H02939, 21H03733, and 21H03736), Early-Career Scientists (23K13689), and Challenging Exploratory Research (22K18997) from Japan Society for the Promotion of Science. The Cooperative Research Project of Research Center for Biomedical Engineering, Nippon Sheet Glass Foundation, Terumo Life Science Foundation, KRF foundation, Tokuyama Science Foundation, Iketani Science and Technology Foundation, and Foundation for Nara Institute of Science and Technology are also acknowledged.

References

Alexandrov, B.S., Ianakiev, K.D., Littlewood, P.B., 2008. Branching transport model of NaI(Tl) alkali-halide scintillator. Nucl. Instruments Methods Phys. Res. Sect. A Accel. Spectrometers, Detect. Assoc. Equip. 586, 432–438. https://doi.org/10.1016/j.nima.2007.12.010.

Bartram, R.H., Kappers, L.A., Hamilton, D.S., Lempicki, A., Brecher, C., Glodo, J., Gaysinskiy, V., Ovechkina, E.E., 2006. Suppression of afterglow in CsI:Tl by codoping with Eu^{2+} - II: theoretical model. Nucl. Instruments Methods Phys. Res. Sect. A Accel. Spectrometers, Detect. Assoc. Equip. 558, 458–467. https://doi.org/10.1016/j.nima.2005.11.051.

Bloser, P.F., Legere, J.S., Bancroft, C.M., McConnell, M.L., Ryan, J.M., 2014. Scintillators with silicon photomultiplier readouts for high-energy astrophysics and heliophysics. Sp. Telesc. Instrum. 2014 Ultrav. to Gamma Ray. 9144, 914414 https://doi.org/10.1117/12.2056906.

Cherepy, N.J., Kuntz, J.D., Seeley, Z.M., Fisher, S.E., Drury, O.B., Sturm, B.W., Hurst, T. A., Sanner, R.D., Roberts, J.J., Payne, S.A., 2010. Transparent ceramic scintillators for gamma spectroscopy and radiography. Hard X-Ray, Gamma-Ray, Neutron Detect. Phys XII (7805), 78050I. https://doi.org/10.1117/12.862503.

Ershov, B.G., Janata, E., Henglein, A., 1994. Mixed-metal clusters in aqueous solution: reactions of Tl^{2+} with Ag^{+}, Cd^{2+}, and Pb^{2+} and of Zn^{+} with Tl^{+}. J. Phys. Chem. 98, 10891–10894. https://doi.org/10.1021/j100093a034.

Greskovich, C., Duclos, S., 1997. Ceramic scintillators. Annu. Rev. Mater. Sci. 27, 69–88. https://doi.org/10.1146/annurev.matsci.27.1.69.

Hofstadter, R., 1948. Alkali halide scintillation counters [4]. Phys. Rev. 74, 100–101. https://doi.org/10.1103/PhysRev.74.100.

Hofstadter, R., McIntyre, J.A., 1950. Gamma-ray measurements with NaI(T1) crystals [2]. Phys. Rev. 79, 389–391. https://doi.org/10.1103/PhysRev.79.389.2.

Ishikane, M., 1974. Decay times of thallous dimer emisssions in NaI(Tl). J. Phys. Soc. Japan. 36, 1572–1576. https://doi.org/10.1143/JPSJ.36.1572.

Ishikane, M., Kawanishi, M., 1975. The scintillation process of NaI (Tl). Jpn. J. Appl. Phys. 14, 64–69. https://doi.org/10.1143/JJAP.14.64.

Kato, T., Okada, G., Fukuda, K., Yanagida, T., 2017. Development of BaF_2 transparent ceramics and evaluation of the scintillation properties. Radiat. Meas. 106, 140–145. https://doi.org/10.1016/j.radmeas.2017.03.032.

Kato, T., Kawano, N., Okada, G., Kawaguchi, N., Fukuda, K., Yanagida, T., 2018. Scintillation properties of SrF_2 translucent ceramics and crystal. Optik 168, 956–962. https://doi.org/10.1016/j.ijleo.2018.04.082.

Kimura, H., Nakamura, F., Kato, T., Nakauchi, D., Okada, G., Kawaguchi, N., Yanagida, T., 2018. Optical and scintillation properties of Tl-doped CsBr transparent ceramics produced by spark plasma sintering. J. Mater. Sci. Mater. Electron. 29, 8498–8503. https://doi.org/10.1007/s10854-018-8863-0.

Kimura, H., Kato, T., Nakauchi, D., Koshimizu, M., Kawaguchi, N., Yanagida, T., 2019. Vacuum-UV-excited photoluminescence and scintillation properties of CsCl transparent ceramics and single crystal. Sensor. Mater. 31, 1265–1271. https://doi.org/10.18494/SAM.2019.2186.

Kubota, S., Shiraishi, F., Takami, Y., 1998. Decay curves of NaI(Tl) scintillators with different Tl^{+} concentrations under excitation of electorons. Alpha Paticles and Fission Fragments 68, 291–297. https://doi.org/10.1143/JPSJ.68.291.

Lecoq, P., 2016. Development of new scintillators for medical applications. Nucl. Instruments Methods Phys. Res. Sect. A Accel. Spectrometers, Detect. Assoc. Equip. 809, 130–139. https://doi.org/10.1016/j.nima.2015.08.041.

Matsubara, T., Yanagida, T., Kawaguchi, N., Nakano, T., Yoshimoto, J., Sezaki, M., Takizawa, H., Tsunoda, S.P., ichiro Horigane, S., Ueda, S., Takemoto-Kimura, S., Kandori, H., Yamanaka, A., Yamashita, T., 2021. Remote control of neural function by X-ray-induced scintillation. Nat. Commun. 12 https://doi.org/10.1038/s41467-021-24717-1.

Messaoudi, I.S., Zaoui, A., Ferhat, M., 2015. Band-gap and phonon distribution in alkali halides. Phys. Status Solidi Basic Res. 252, 490–495. https://doi.org/10.1002/pssb.201451268.

Murray, R.B., Meyer, A., 1961. Scintillation response of activated inorganic crystals to various charged particles. Phys. Rev. 122, 815–826. https://doi.org/10.1103/PhysRev.122.815.

Nagata, S., Fujiwara, K., Nishimura, H., 1990. Dynamical aspects of excitons in NaI. J. Lumin. 47, 147–157. https://doi.org/10.1016/0022-2313(90)90026-8.

Paepen, J., Peerani, P., Schillebeeckx, P., Tomanin, A., Wynants, R., 2013. Use of a CAEN Digitiser for Nuclear Safeguards and Security Applications with a Scintillator Detector. https://doi.org/10.2787/87780.

Phenomena, E.L.D., Fontana, M.P., Van Sciver, W.J., 1953. Energy transfer and optical properties of Tl^{+} centers in NaI(Tl) crystals. Phys. Rev. 168, 960–964. https://doi.org/10.1103/PhysRev.168.960.

Robertson, J.C., Lynch, J.G., 1961. The luminescent decay of various crystals for particles of different ionization density. Proc. Phys. Soc. 77, 751–756. https://doi.org/10.1088/0370-1328/77/3/326.

Sailer, C., Lubsandorzhiev, B., Strandhagen, C., Jochum, J., 2012. Low temperature light yield measurements in NaI and NaI(Tl). Eur. Phys. J. C 72, 1–4. https://doi.org/10.1140/epjc/s10052-012-2061-7.

Seeley, Z.M., Cherepy, N.J., Payne, S.A., 2013. Homogeneity of Gd-based garnet transparent ceramic scintillators for gamma spectroscopy. J. Cryst. Growth 379, 79–83. https://doi.org/10.1016/j.jcrysgro.2012.11.042.

Shiran, N.V., Gektin, A.V., Boyarintseva, Y., Vasyukov, S., Boyarintsev, A., Pedash, V., Tkachenko, S., Zelenskaya, O., Kosinov, N., Kisil, O., Philippovich, L., 2010. Eu doped and eu, Tl co-doped NaI scintillators. IEEE Trans. Nucl. Sci. 57, 1233–1235. https://doi.org/10.1109/TNS.2010.2048578.

Sibczyński, P., Moszyński, M., Szczęśniak, T., Czarnacki, W., 2012. Study of NaI(Tl) scintillator cooled down to liquid nitrogen temperature. J. Instrum. 7 https://doi.org/10.1088/1748-0221/7/11/P11006.

Takahashi, K., Kimura, H., Nakauchi, D., Kato, T., Kawaguchi, N., Yanagida, T., 2020. Photoluminescence and scintillation properties of Ce-doped $CaBr_2$ crystals. Jpn. J. Appl. Phys. 59 https://doi.org/10.35848/1347-4065/abb5c0.

Van Eijk, C.W.E., 2003. Inorganic scintillators in medical imaging detectors. Nucl. Instruments Methods Phys. Res. Sect. A Accel. Spectrometers, Detect. Assoc. Equip. 509, 17–25. https://doi.org/10.1016/S0168-9002(03)01542-0.

Van Sciver, W., 1956. Alkali halide scintillators. IRE Trans. Nucl. Sci. 3, 39–50. https://doi.org/10.1109/TNS2.1956.4315545.

Watanabe, K., Yanagida, T., Fukuda, K., Koike, A., Aoki, T., Uritani, A., 2015. Portable neutron detector using Ce:$LiCaAlF_6$ scintillator. Sensor. Mater. 27, 269–275. https://doi.org/10.18494/sam.2015.1093.

Weber, M.J., 2002. Inorganic scintillators: today and tomorrow. J. Lumin. 100, 35–45. https://doi.org/10.1016/S0022-2313(02)00423-4.

Yanagida, T., 2016. Ionizing radiation induced emission: scintillation and storage-type luminescence. J. Lumin. 169, 544–548. https://doi.org/10.1016/j.jlumin.2015.01.006.

Yanagida, T., 2018. Inorganic scintillating materials and scintillation detectors. Proc. Japan Acad. Ser. B Phys. Biol. Sci. 94, 75–97. https://doi.org/10.2183/pjab.94.007.

Yanagida, T., Takahashi, H., Ito, T., Kasama, D., Enoto, T., Sato, M., Hirakuri, S., Kokubun, M., Makishima, K., Yanagitani, T., Yagi, H., Shigeta, T., Ito, T., 2005. Evaluation of properties of YAG (Ce) ceramic scintillators. IEEE Trans. Nucl. Sci. 52, 1836–1841. https://doi.org/10.1109/TNS.2005.856757.

Yanagida, T., Fujimoto, Y., Yokota, Y., Kamada, K., Yanagida, S., Yoshikawa, A., Yagi, H., Yanagitani, T., 2011. Comparative study of transparent ceramic and single crystal Ce doped LuAG scintillators. Radiat. Meas. 46, 1503–1505. https://doi.org/10.1016/j.radmeas.2011.03.039.

Yanagida, T., Fujimoto, Y., Kamada, K., Totsuka, D., Yagi, H., Yanagitani, T., Futami, Y., Yanagida, S., Kurosawa, S., Yokota, Y., Yoshikawa, A., Nikl, M., 2012. Scintillation properties of transparent ceramic pr:LuAG for different pr concentration. IEEE Trans. Nucl. Sci. 59, 2146–2151. https://doi.org/10.1109/TNS.2012.2189583.

Yanagida, T., Fujimoto, Y., Kurosawa, S., Kamada, K., Takahashi, H., Fukazawa, Y., Nikl, M., Chani, V., 2013a. Temperature dependence of scintillation properties of bright oxide scintillators for well-logging. Jpn. J. Appl. Phys. 52 https://doi.org/10.7567/JJAP.52.076401.

Yanagida, T., Kamada, K., Fujimoto, Y., Yagi, H., Yanagitani, T., 2013b. Comparative study of ceramic and single crystal Ce:GAGG scintillator. Opt. Mater. 35, 2480–2485. https://doi.org/10.1016/j.optmat.2013.07.002.

Yanagida, T., Fujimoto, Y., Ito, T., Uchiyama, K., Mori, K., 2014a. Development of X-ray-induced afterglow characterization system. Appl. Phys. Express. 7, 8–11. https://doi.org/10.7567/APEX.7.062401.

Yanagida, T., Fujimoto, Y., Watanabe, K., Fukuda, K., Kawaguchi, N., Miyamoto, Y., Nanto, H., 2014b. Scintillation and optical stimulated luminescence of Ce-doped CaF_2. Radiat. Meas. 71, 162–165. https://doi.org/10.1016/j.radmeas.2014.03.020.

Yoshikawa, Y., Kato, T., Nakauchi, D., Kawaguchi, N., Yanagida, T., 2022. Scintillation property of undoped NaI transparent ceramics. Jpn. J. Appl. Phys. 61 https://doi.org/10.35848/1347-4065/ac88ab.